ISSN 2755-3531

Vol. 45, no. 6 **Journal of Conchology** 29 July 2026

Published by the Conchological Society of Great Britain and Ireland, established 1874

Taxonomic revision of *Phalium flammiferum breviculum* Tsi & Ma, 1980 (Gastropoda: Cassidae): elevation to species rank

Xing-Xiao Wang[1,2,3] & Shu-Qian Zhang[1,4]

1 *Laboratory of Marine Organism Taxonomy and Phylogeny, Shandong Province Key Laboratory of Marine Biodiversity and Bio-resource Sustainable Utilization, Institute of Oceanology, Chinese Academy of Sciences, Qingdao 266000, China*

2 *College of Life Sciences, Capital Normal University, Beijing 100048, China*

X-XW: *0009-0005-8009-4346*; S-QZ: *0000-0002-1521-5317*

Corresponding author: *Shuqian Zhang (zsqtaxon@qdio.ac.cn)*

Abstract. *Phalium flammiferum breviculum* Tsi & Ma, 1980 has long been regarded as a subspecies of *Phalium flammiferum* (Röding, 1798) or sometimes treated as its synonym. In this study, integrative morphological and molecular phylogenetic analyses of *P. flammiferum breviculum* Tsi & Ma, 1980 and *P. flammiferum flammiferum* (Röding, 1798) from Chinese waters demonstrate that they represent two distinct species. Morphologically, the two species differ primarily in discrete characters of shell sculpture, particularly in the number of spiral cords and varices. Geometric morphometric analyses and mapping of landmark configurations onto the phylogeny indicate that variation in shell outline is largely continuous and only weakly associated with phylogenetic relationships. Phylogenetic analyses reconstructed by Bayesian inference using concatenated mitochondrial (COI) and nuclear (28S rRNA) genes and species delimitation analysis (ASAP) support the separation of the two species. Herein, we formally elevate *Phalium flammiferum breviculum* Tsi & Ma, 1980 to species rank.

Key words. China Seas, Yellow Sea Cold Water Mass, Mollusca, species distinction

ZooBank. urn:lsid:zoobank.org:pub:6D08158A-DC9F-485D-A93C-F7CE156B2219

DOI. https://doi.org/10.61733/jconch/4579

Introduction

Cassidae Latreille, 1825 is a moderately diverse family of marine gastropods, comprising over 100 described species distributed worldwide in tropical and subtropical waters, ranging from the intertidal zone to the deep sea. Traditional taxonomic classification of this family has primarily relied on shell morphology (e.g. shape, sculpture, colouration), but intraspecific variation and convergent evolution frequently result in taxonomic ambiguities at both the specific and the generic level (Beu 2008).

Phalium flammiferum (Röding, 1798) exhibits a relatively narrow distribution in Japan, China, and the Philippines. This species is characterised by a large, oval shell with a smooth surface marked with longitudinal brown stripes. In Chinese waters, this species has been recorded from various localities by different authors. Tsi & Ma (1980) recognised two distinct morphotypes of *P. flammiferum*: the northern morphotype from the Bohai Sea and Yellow Sea, and the southern morphotype from the East China Sea and the South China Sea. The two morphotypes differ primarily in the number of spiral cords on the shell and their geographic distributions (with a small range overlap near Changjiang Estuary). They described the northern morphotype as a subspecies, *P. strigatum breviculum* Tsi & Ma, 1980. This taxonomic treatment was subsequently accepted by some authors (Qi *et al.* 1989; Zhang & Ma 2004; Zhang *et al.* 2016), while others considered this subspecies invalid (Sun *et al.* 2012; Verbinnen *et al.* 2016), leading to taxonomic controversy. However, the taxonomic status of *P. flammiferum breviculum* has not been rigorously evaluated using integrative morphological and molecular evidence.

To assess the taxonomic status of *P. flammiferum breviculum*, we collected fresh specimens of *P. flammiferum s.l.* from Chinese waters across the Yellow Sea, East China Sea, and the South China Sea. Detailed morphological comparisons were performed based on shells and radulae, supplemented by molecular analyses of the COI and 28S rRNA genes. In addition, the reliability of shell outline as a diagnostic character remains uncertain, as variation of shell shape in cassids

may be continuous or influenced by intraspecific variability. Geometric morphometric approaches provide a quantitative framework to assess variation in shell shape and to evaluate the extent to which different aspects of shell morphology contribute to species delimitation. Furthermore, mapping shell landmark configurations onto the molecular phylogeny allows us to evaluate whether variation in shell shape corresponds to phylogenetic relationships. This study aims to reassess the taxonomic status of *P. flammiferum breviculum* using integrative morphological and molecular evidence.

Materials and Methods

Specimen sampling and preservation. Materials examined in this study include the type specimens of *Phalium flammiferum breviculum* deposited in the Marine Biological Museum of Chinese Academy of Sciences (MBMCAS) and newly collected specimens from three localities: the Yellow Sea (covering the type locality), East China Sea, and the South China Sea. All newly collected specimens were preserved in 99.9% ethanol and deposited in MBMCAS.

Morphological analyses. The shells were examined using light microscopy and photographed with a digital camera. SEM examinations of radular characters were performed on two Yellow Sea specimens (MBM288432, MBM288442), one East China Sea specimen (MBM288426), and one South China Sea specimen (MBM288422). The radulae were cleaned with 10% NaOH for 30 min, rinsed in distilled water, air-dried, coated with gold, and examined under SEM at an accelerating voltage of 5 kV.

Geometric morphometric analyses. Specimens were assigned to species groups according to the molecular phylogenetic results and taxonomic identifications established in the present study, and these predefined groups were then used for visualization and comparison in PCA plots. We used geometric morphometric analyses to compare shell shapes of three taxa in genus *Phalium*, based on shell photographs of examined specimens in the present study, as well as published photographs from Verbinnen *et al.* (2016). Only adult shells photographed in comparable apertural view and without obvious perspective distortion were included.

Landmarks and semi-landmarks were collected from shell images using tpsDig2 (Rohlf 2015). A total of 59 shells were included in the geometric morphometric analysis, comprising 29 specimens referable to *P. flammiferum breviculum*, 16 specimens referable to *P. flammiferum flammiferum*, and 14 specimens referable to *P. muangmani* Raybaudi Massilia & Prati Musetti, 1995 (Table 1). For each shell, 20 landmarks were digitised, including six fixed landmarks and 14 semi-landmarks. The landmark configuration is illustrated in Figure 1.

Landmark coordinates were imported into MorphoJ v. 1.08.02 (Klingenberg 2011), where a Procrustes fit was performed, followed by generation of a covariance matrix and principal component analysis (PCA). Patterns of shell shape variation among the three taxa were examined using PCA under different landmark configurations. PCA scatter plots were visualised with 95% confidence ellipses to illustrate morphospace occupation and the extent of overlap among taxa.

Mapping of variation of shell shape onto the phylogeny. To further evaluate whether variation in shell outline corresponds to phylogenetic relationships, we mapped landmark configurations onto the molecular phylogeny. This analysis was restricted to specimens for which both molecular data and comparable shell images were available. The concate-

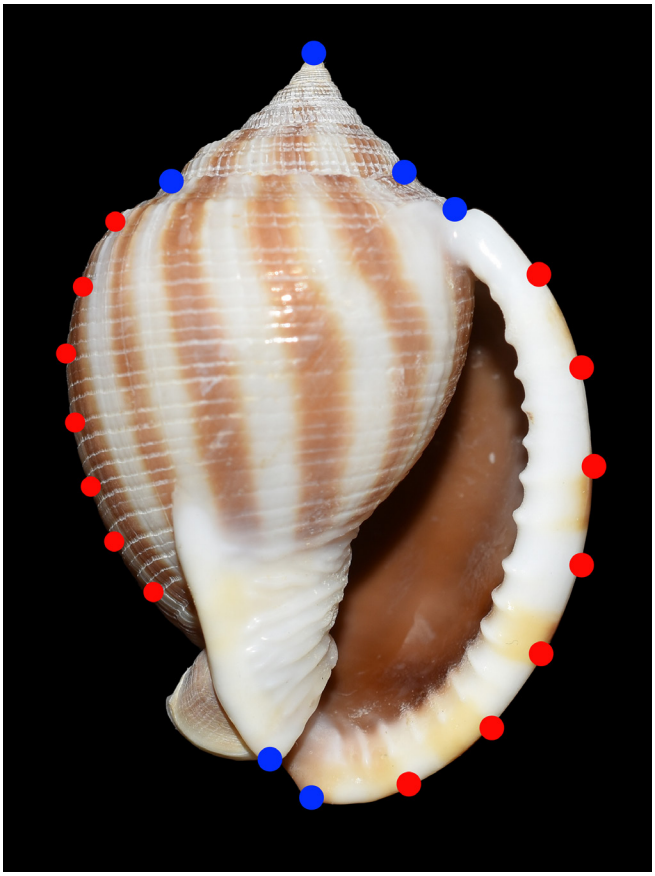

Figure 1. Landmark configuration used for geometric morphometric analyses of shell shape in apertural view. Blue dots indicate fixed landmarks, and red dots indicate semi-landmarks.

Table 1. Specimens included in geometric morphometric analysis.

Specimen ID	Species	Locality	Source
MBM288428	*P. breviculum*	Yellow Sea, off Dalian	This study
MBM288430	*P. breviculum*	Yellow Sea, off Dalian	This study
MBM288431–MBM288434	*P. breviculum*	Yellow Sea, off Qingdao	This study
MBM288441–MBM288444	*P. breviculum*	Bohai Sea, off Laizhou	This study
WXC3316A–WXC3316R	*P. breviculum*	Yellow Sea, off Qingdao	This study
Verbinnen *et al.* 2016: pl. 55 fig. 7a	*P. breviculum*	Yellow Sea	Published image
MBM288422–MBM288423	*P. flammiferum*	South China Sea	This study
MBM288424–MBM288426	*P. flammiferum*	East China Sea	This study
WXC1145A–WXC1145E	*P. flammiferum*	South China Sea	This study
Verbinnen *et al.* 2016: pl. 55 fig. 2a	*P. flammiferum*	Vietnam, Nha Trang	Published image
Verbinnen *et al.* 2016: pl. 55 fig. 3a	*P. flammiferum*	Japan, off Kii Peninsula	Published image
Verbinnen *et al.* 2016: pl. 55 fig. 4a	*P. flammiferum*	East China Sea	Published image
Verbinnen *et al.* 2016: pl. 55 fig. 5a	*P. flammiferum*	East China Sea	Published image
Verbinnen *et al.* 2016: pl. 55 fig. 6a	*P. flammiferum*	Japan, off Kii Peninsula	Published image
Verbinnen *et al.* 2016: pl. 55 fig. 8a	*P. flammiferum*	East China Sea	Published image
MBM288435–MBM288440, MBM28445	*P. muangmani*	East China Sea	This study
Verbinnen *et al.* 2016: pl. 54 fig. 1a	*P. muangmani*	East China Sea	Published image
Verbinnen *et al.* 2016: pl. 54 fig. 2a	*P. muangmani*	East China Sea	Published image
Verbinnen *et al.* 2016: pl. 54 fig. 3a	*P. muangmani*	East China Sea	Published image
Verbinnen *et al.* 2016: pl. 54 fig. 4a	*P. muangmani*	Thailand, off Phuket Island	Published image
Verbinnen *et al.* 2016: pl. 54 fig. 5a	*P. muangmani*	Thailand, off Phuket Island	Published image
Verbinnen *et al.* 2016: pl. 54 fig. 6a	*P. muangmani*	China, off Xiamen	Published image
Verbinnen *et al.* 2016: pl. 54 fig. 8a	*P. muangmani*	East China Sea	Published image

nated COI + 28S phylogeny was pruned to retain only these specimens. The same Procrustes-aligned landmark configurations used in the geometric morphometric analyses were imported into TNT v. 1.6 (Goloboff and Morales 2023) and optimised onto the pruned phylogeny under a parsimony framework. Ancestral landmark configurations were reconstructed for internal nodes and visualised together with terminal configurations to assess the pattern of shell shape change across the tree.

Molecular analysis. Seven newly collected specimens, including two from the Yellow Sea, three from the East China Sea, and two from the South China Sea, were subjected to molecular analysis. Genomic DNA of five specimens was extracted with the Column Genomic DNA Isolation Kit (Beijing TIANGEN, China) according to the manufacturer's instructions. The COI gene was amplified by polymerase chain reaction (PCR) using the primers LCO1490 and HCO2198 (Folmer *et al.* 1994), the 28S rRNA was amplified by the primers 28SC1 and 28SD2 (Jovelin & Justine 2001). PCR reactions were performed in a total volume of 25 µl, including 12.5 µl 2×Hieff PCR Master Mix, 9.5 µl ddH_2O, and 0.5 µl of both forward and reverse PCR primers, and 2 µl DNA. The thermal cycling was performed under the following conditions: initial denaturation at 95 °C for 3 min; 35 cycles of denaturation at 95 °C for 30 s, annealing at 42 °C for COI and 42–45 °C for 28S for 45 s, and extension at 72 °C for 60 s; followed by a final extension at 72 °C for 10 min. PCR products were verified on a GelRed-stained 1.5% agarose gel and sequenced by Biotechnology Company. For two other specimens (MBM288422 and MBM288430) for which conventional primer-based amplification of the COI and 28S rRNA genes failed, next-generation sequencing (NGS) was performed. Sequencing libraries were generated using DNBSEQ-T7 platform following manufacturer's recommendations and index codes were added to attribute sequences to each sample. Briefly, the DNA sample was fragmented by sonication to a size of 350 bp, then DNA fragments were end polished, A-tailed, and ligated with the full-length adapter for sequencing with further PCR amplification. At last, PCR products were purified (AMPure XP system) and libraries were analysed for size distribution by Agilent2100 Bioanalyzer and quantified using real-time PCR. The libraries constructed above were sequenced by

Table 2. Species of Cassidae and GenBank accession numbers of sequences used in the present study.

Species	Voucher	COI	28S	References
Casmaria boblehmani	IM-2007-33625	KC970027	MH571179	Fedosov *et al.* 2014
Casmaria erinaceus	IM-2007-33621	KC970029	—	Fedosov *et al.* 2014
Casmaria erinaceus	isolate Casm.1	KC505363	—	Fedosov *et al.* 2014
Casmaria ponderosa	isolate Casm.2	KC505362	—	Fedosov *et al.* 2014
Cassis cornuta	AIWC/RES/12/24/0479	PV799788	—	Madhumita *et al.*, unpublished
Cassis fimbriata	IM-2009-23323	MH581307	MH571180	Strong *et al.* 2019
Cassis flammea	IM-2013-19516	MH581308	—	Strong *et al.* 2019
Cassis madagascariensis	IM-2013-19553	MH581309	MH571181	Strong *et al.* 2019
Cypraecassis rufa	IM-2013-40295	MH581316	MH571184	Strong *et al.* 2019
Cypraecassis rufa	IM-2013-40297	MH581315	—	Strong *et al.* 2019
Cypraecassis testiculus	IM-2013-19567	MH581317	MH571185	Strong *et al.* 2019
Dalium barbouri	IM-2013-61106	MH581331	MH571194	Strong *et al.* 2019
Dalium solidum	IM-2013-56835	MH581318	—	Strong *et al.* 2019
Echinophoria kurodai	IM-2007-33650	MH581328	—	Strong *et al.* 2019
Echinophoria wyvillei	IM-2007-33639	MH581329	MH571192	Strong *et al.* 2019
Echinophoria wyvillei	IM-2007-33647	MH581330	MH571193	Strong *et al.* 2019
Galeodea bituminata	IM-2007-33627	MH581335	MH571198	Strong *et al.* 2019
Galeodea bituminata	IM-2007-34694	MH581336	—	Strong *et al.* 2019
Galeodea echinophora	IM-2009-7834	MH581337	MH571199	Strong *et al.* 2019
Oocorys verrillii	IM-2007-33652	MH581349	—	Strong *et al.* 2019
Phalium flammiferum breviculum	MBM288432	PZ211659	PZ299328	This study
Phalium flammiferum breviculum	MBM288431	PZ211660	PZ299329	This study
Phalium flammiferum breviculum	MBM288430	PZ211661	PZ299330	This study
Phalium flammiferum breviculum	MBM288442	PZ299325	PZ299331	This study
Phalium flammiferum breviculum	isolate XA10	JF693410	—	Sun *et al.* 2012
Phalium flammiferum flammiferum	HNWI-2238	OQ828224	—	Zheng unpublished
Phalium flammiferum flammiferum	MBM288424	PZ211662	—	This study
Phalium flammiferum flammiferum	MBM288425	PZ211663	PZ299332	This study
Phalium flammiferum flammiferum	MBM288426	PZ211664	PZ299333	This study
Phalium flammiferum flammiferum	MBM288422	PZ211666	PZ299334	This study
Phalium flammiferum flammiferum	MBM288423	PZ211665	PZ299335	This study
Phalium flammiferum flammiferum	MBM288446	PZ299326	PZ299336	This study
Phalium flammiferum flammiferum	MBM288447	PZ299327	PZ299337	This study
Phalium glaucum	Vt057	LC738360	LC738244	Setiamarga *et al.* 2025
Phalium glaucum	Vt026	LC738336	—	Setiamarga *et al.* 2025
Phalium muangmani	MBM288435	PZ211667	PZ299338	This study
Phalium muangmani	MBM288436	PZ211668	PZ299339	This study
Sconsia alexarthuri	IM-2013-61442	MH581368	MH571220	Strong *et al.* 2019
Sconsia grayi	IM-2013-60869	—	MH571221	Strong *et al.* 2019
Semicassis bisulcata	IM-2007-34811	MH581369	MH571222	Strong *et al.* 2019
Semicassis bisulcata	IM-2007-34812	MH581370	MH571223	Strong *et al.* 2019
Semicassis sp.	IM-2007-33622	MH581371	MH571225	Strong *et al.* 2019
Semicassis bulla	IM-2007-33618	—	MH571224	Strong *et al.* 2019
Charonia tritonis	IM-2007-36517	MH581312	MH571182	Strong *et al.* 2019
Charonia variegata	IM-2013-19537	MH581313	MH571183	Strong *et al.* 2019

DNBSEQ-T7 platform and 150-bp paired-end reads were generated with insert size around 350 bp. To make sure reads reliable and without artificial bias, raw reads of fast format was processed through a series of quality control (QC) procedures in-house C scripts. For each specimen, the COI and 28S rRNA genes were de novo assembled from raw NGS reads using NOVOPlasty software (Dierckxsens *et al.* 2017), with COI and 28S rRNA fragments from closely related species used as the seed.

Phylogenetic reconstruction. Obtained sequences and additional sequences of cassid species retrieved from GenBank were used for phylogenetic analyses (Table 2). Two species of Charoniidae were used as outgroup to root the tree. Sequences were aligned using MAFFT v. 7 (Katoh & Standley 2013) with the G-INS-i algorithm. Gap sites of COI were removed with trimAl (Capella-Gutiérrez *et al.* 2009) using "-cons 10.0 -gt 0.7 -st 0.0 -w 1.0" command. Ambiguously aligned 28S rRNA fragments were removed using Gblocks (Talavera & Castresana 2007). Sequences from the same individual were concatenated into one single alignment (1204 bp). Phylogenetic analyses were performed on three datasets: concatenated COI and 28S rRNA sequences, and separate single-gene alignments of COI and 28S rRNA, respectively. ModelFinder (Kalyaanamoorthy *et al.* 2017) was used to select the best-fit model using BIC criterion (concatenated dataset: GTR+I+G4 for both COI and 28S rRNA; single-gene datasets: GTR+I+G4 for COI and GTR+I for 28S). Bayesian Inference phylogenies were inferred using MrBayes v. 3.2.6 (Ronquist *et al.* 2012) under the best-fit model (2 parallel runs, 5, million generations), in which the initial 25% of sampled data were discarded as burn-in; split frequencies were <0.01 before the analyses were terminated. Convergence of each run was evaluated using Tracer v. 1.7.1 (Rambaut *et al.* 2018) to check that all effective sample size values exceeded 200. Results were visualised by tvBOT (Xie *et al.* 2023). The *p*-distances within and among each species grouping were estimated with MEGA 6 (Tamura *et al.* 2013).

Species delimitation. For species delimitation, monophyletic species concept (a species is the smallest monophyletic unit that can be distinguished) was adopt (De Queiroz 2007). In addition to phylogenetic analyses, the Assemble Species by Automatic Partitioning (ASAP) (Puillandre *et al.* 2021) method was used to explore putative species partitions within *Phalium*. The alignment from the fast-evolving COI gene was uploaded to the online server of ASAP (https://spartexplorer.mnhn.fr/). The analyses were performed with the model of Jukes-Cantor (JC69) with default settings.

Results

Geometric morphometric analyses

Geometric morphometric analyses based on different landmark configurations revealed varying degrees of morphospace separation among the three *Phalium* species (Fig. 2). Principal component analysis (PCA) based on fixed landmarks showed the clearest differentiation among taxa (Fig. 2B), with the first two principal components explaining 64.420% and 27.474% of the total shape variation, respectively. The three species exhibited distinct tendencies in morphospace, although some overlap remained.

In contrast, PCA based on semi-landmarks showed substantial overlap among taxa (Fig. 2C, D). The combined dataset of fixed and semi-landmarks (Fig. 2A) produced intermediate results, with reduced separation compared to fixed landmarks alone. Overall, the degree of separation among groups varied depending on landmark configuration, with fixed landmarks capturing more pronounced interspecific differences than semi-landmarks.

Mapping of the Procrustes-aligned landmark configurations onto the pruned molecular phylogeny revealed no clear correspondence between shell outline variation and phylogenetic relationships (Supplemental Materials, Fig. S1). The reconstructed landmark configurations at internal nodes and the terminal configurations indicate that changes in shell outline are generally gradual and subtle across the sampled *Phalium* species. Although *P. breviculum*, *P. flammiferum* and *P. muangmani* are separated in the molecular phylogeny, their shell outline configurations are broadly similar and do not show distinct species-specific transformations. This result is consistent with the PCA results, suggesting that shell outline has limited discriminatory resolution and limited phylogenetic signal in the present dataset.

Phylogenetic analyses

Both the Bayesian inference (BI) phylogenetic trees based on the concatenated COI and 28S genes and the single COI gene supported the monophyly of the genus *Phalium*. In the concatenated COI and 28S tree, *P. flammiferum breviculum* formed a distinct monophyletic clade separated from all other congeners including *P. flammiferum flammiferum* (PP = 1; Figure 3). The single-gene COI tree (Supplemental Materials, Fig. S2) recovered *P. flammiferum breviculum* as the sister clade to *P. flammiferum flammiferum*. By contrast, the 28S-only BI tree (Supplemental Materials, Fig. S3) failed to resolve the monophyly of *Phalium*, as well as the monophyly of the two taxa. In this 28S tree, individuals of *P. flam-*

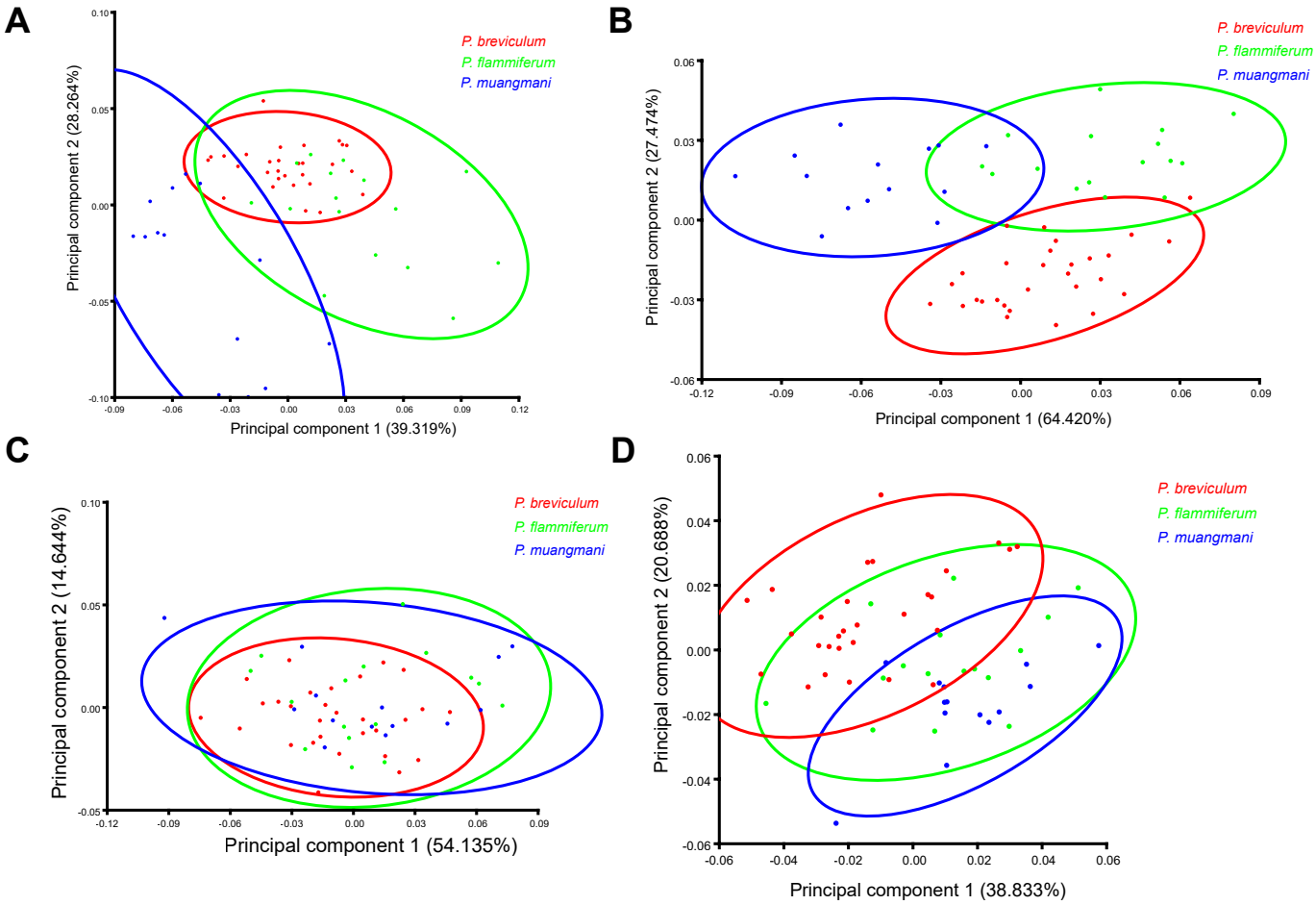

Figure 2. Principal component analyses (PCA) of ventral shell shape in three *Phalium* species based on different landmark configurations. **A**, combined fixed and semi-landmarks. **B**, fixed landmarks only. **C**, left semi-landmarks. **d**, right semi-landmarks. Ellipses represent 95% confidence intervals.

miferum breviculum clustered with *Echinophoria wyvillei*, while *P. flammiferum flammiferum* grouped with *P. muangmani*.

Species delimitation

The ASAP analysis of the available COI sequences resulted in the delimitation of four species with the lowest score (the most supported partition scheme) (Supplemental Materials, Fig. S4). The inferred threshold distance is 3.8% (Fig. 4). These groups correspond to clades recovered by BI analysis.

With available molecular data, analysis of a 562-bp fragment of the COI gene yielded a 6.8%–8.2% pairwise distance between *P. flammiferum breviculum* and *P. flammiferum flammiferum*, a divergence much higher than the known intraspecific variation of *Phalium* spp. (0–2%). The pairwise distance between *P. flammiferum breviculum* and other congeners ranged from 7.0 to 8.9%.

These results provide additional support for recognizing *Phalium flammiferum breviculum* as a distinct species. Pairwise COI *p*-distances among the examined *Phalium* species are summarised in Table 3.

Systematics

Superfamily Tonnoidea Suter, 1913 (1825)

Family Cassidae Latreille, 1825

Genus *Phalium* Link, 1807

Type species. *Buccinum glaucum* Linnaeus, 1758 (type by subsequent designation).

Phalium flammiferum (Röding, 1798)

Figures 5A–G, 6A–F

Buccinum strigatum Gmelin 1791: 3477, no. 179.
Cassis flammifera Röding 1798: 31, no. 377.
Cassis strigata (Gmelin, 1791)—Yen 1933: 63.
Phalium (*Phalium*) *strigatum strigatum* (Gmelin, 1791)—Tsi

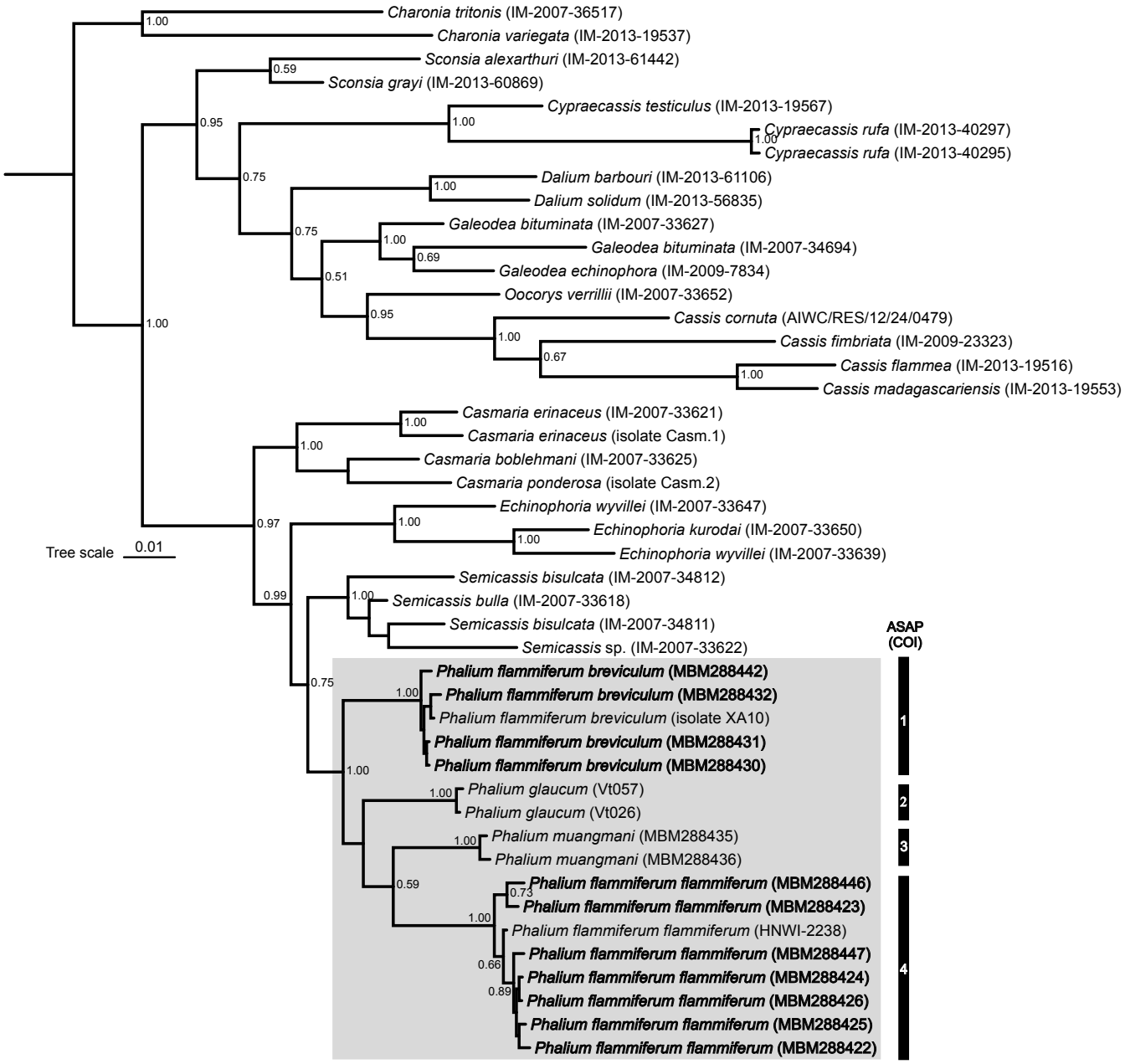

Figure 3. Phylogenetic tree of Cassidae inferred by Bayesian analysis (BI) based on concatenated COI and 28S rRNA genes. Numbers adjacent to nodes refer to BI posterior probability (>0.5); numbers in the vertical black bars indicate the results of ASAP species delimitations.

& Ma 1980: 86, pl. 2 figs 1, 2.

Phalium (*Phalium*) *flammiferum* (Röding, 1798)—Zhang & Ma 2004: 45, text fig. 24, pl. 1 fig. 3.

Phalium (*Bezoardicella*) *flammiferum* (Röding, 1798)—Okutani 2000: 277, pl. 137 fig. 19.

Phalium flammiferum (Röding, 1798)—Poppe 2008: 580, pl. 235 fig. 6; Verbinnen *et al*. 2016: 53, pl. 55 figs 1–6, 8; Okutani 2017: 870, pl. 157 (live specimen, not numbered).

Material examined. 2 specimens (MBM288422 & MBM 288423), South China Sea, 23° 05′ N 117° 01′ E, 34 m depth, broken shell substrate, 25 October 2024. 5 specimens (MBM 288424–MBM 288426, MBM 288446 & MBM 288447), East China Sea, 26° 30′ N 123° 46′ E, 100–120 m deep, 30 October 2025. 5 specimens (WXC 1145A–WXC 1145E), Xing-Xiao Wang collection, empty shell, South China Sea.

Molecular diagnosis. Among available COI sequences, pairwise COI genetic divergence between *P. flammiferum*

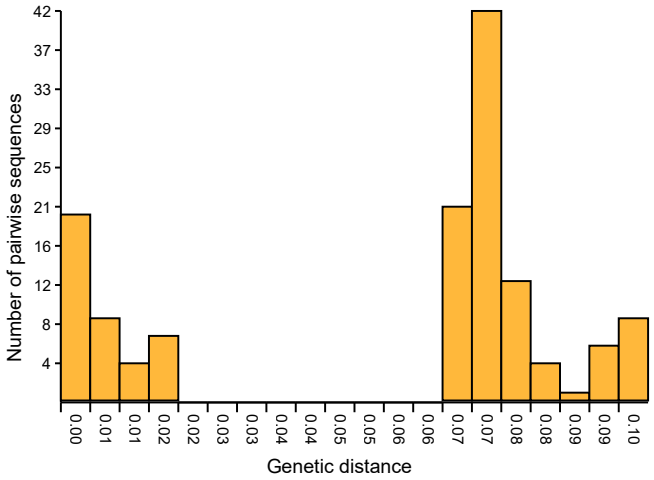

Figure 4. Results of the ASAP analysis showing the distribution of COI pairwise *p*-distances among *Phalium* species.

and other congeners ranges from 6.8% to 10.3%. *Phalium flammiferum* is reliably distinguished from other *Phalium* species by possession of a specific combination of nucleotides in the sequence at sites 114 (C), 153 (G), 165 (G), 174 (G), 309 (G), 324 (C), 327 (C), 354 (C), 372 (A), 420 (C), 423 (G), 450 (G), 453 (C) and 468 (G).

Description. Shell (Fig. 5A–G) of moderate size for genus, subglobose, heavy, and solid. Spire narrowly conical; last whorl well inflated. Protoconch consisting of ~2.5 smooth, evenly convex whorls; teleoconch of 6 whorls. Spiral cords and axial ribs on spire intersecting, giving shell surface a granulose appearance. On last whorl, spiral cords becoming much wider and rather flattened, 18–20 in number; axial sculpture limited to a few growth lines. In addition to spiral cords and axial ribs, shell surface bearing 3–5 well-developed varices. Siphonal canal short and curved. Outer lip thickened, with 19–21 internal denticles; inner lip with well-developed parietal callus, forming a thick plait with tubercles on columella. Umbilicus covered by columellar plait. Shell colour white, adorned with longitudinal, curved, bright brown streaks; outer lip, inner lip, and varices marked with orange bands.

Radula (Fig. 6A–F) formula: 2.1.1.1.2. Central teeth bearing 4–7 long, strong denticles on each side of slightly longer, stronger central cusp. Lateral teeth each with 7–10 long, strong denticles, decreasing in size toward outer margin. Marginal teeth each bearing four denticles on inner edge.

Type locality. Not designated.

Geographic range. In China, this species occurs in the East China Sea, Taiwan, and the South China Sea. It is also distributed in Japan and the Philippines.

Phalium breviculum Tsi & Ma, 1980, stat. nov.

Figures 5H–L, 6G–L, 7

Phalium (*Phalium*) *strigatum breviculum* Tsi & Ma 1980: 87, pl. 2 figs 3, 4—Qi *et al.* 1989: 54, pl. 2 fig. 54; Zhang & Zhang 2015: 12, fig. 39.

Phalium strigatum—Yen 1936: 214, pl. 18, figs 35, 35a; Zhao 1982: 50, pl. 4 fig. 23 (not Gmelin, 1791).

Phalium (*Phalium*) *flammiferum breviculum* Tsi & Ma, 1980—Zhang & Ma 2004: 47, text fig. 26.

Phalium flammiferum—Min 2004: 181, fig. 426 (not Röding 1798); Okutani 2017: pl. 157 fig. 6 (not Röding 1798).

Phalium flammiferum (Röding, 1798)—Verbinnen *et al.* 2016: 53, pl. 55 fig. 7 (as forma *breviculum*).

Phalium strigatum breviculum Tsi & Ma, 1980—Zhang *et al.* 2016: 80, fig. 90.

Material examined. Holotype (MBM 288428), Yellow Sea, off Xiaochangshan Island, Dalian, 8 September, 1956; paratypes, 2 specimens (MBM 288429), Bohai Sea, off Beidaihe, Hebei Province, 3 May, 1950; 1 specimen (MBM 288430), Yellow Sea, off Dalian, 16 November, 2025; 4 specimens (MBM 288431–MBM 288434), Yellow Sea, off Qingdao, 13 December, 2024; 4 specimens (MBM 288441–MBM 288444), Bohai Sea, off Laizhou, 11 April, 2026; 18 specimens (WXC 3316A–WXC 3316R), Xing-Xiao Wang collection, empty shell, Yellow Sea, off Qingdao.

Molecular diagnosis. Among available COI sequences,

Table 3. Estimates of *p*-distances of mitochondrial COI gene among *Phalium* species and studied sequences. Intraspecific distances in bold.

	Maximum distance between and minimum distance within species			
	P. glaucum	*P. flammiferum*	*P. breviculum*	*P. muangmani*
P. glaucum	**0.002**			
P. flammiferum	0.096–0.103	**0.002–0.020**		
P. breviculum	0.070–0.077	0.068–0.082	**0.000–0.004**	
P. muangmani	0.077–0.081	0.076–0.089	0.078–0.084	**0.005**

Figure 5. Type and sequenced specimens of *Phalium*. **A**–**G**, *P. flammiferum* (Röding, 1798): (**A**) MBM288424, East China Sea, 83.3 mm; (**B**) MBM288425, East China Sea, 67.6 mm; (**C**) MBM288426, East China Sea, 63.3 mm; (**D**) MBM288446, East China Sea, 74.0 mm; (**E**) MBM288447, East China Sea, 80.0 mm; (**F**) MBM288423, South China Sea, 72.3 mm; (**G**) MBM288422, South China Sea, 60.8 mm. **H**–**L**, *P. breviculum* Tsi & Ma, 1980: **H**, holotype, MBM288428, Yellow Sea, off Xiaochangshan Island; (**I**) MBM288430, Yellow Sea, off Dalian, 54.0 mm; (**J**) MBM288432, Yellow Sea, off Qingdao, 47.0 mm; (**K**) MBM288431, Yellow Sea, off Qingdao, 45.0 mm; (**L**) MBM288442, Bohai Sea, off Laizhou, 54.6 mm.

pairwise genetic divergence in COI ranges from 6.8% to 8.9% between *P. breviculum* and other members of the genus. *Phalium breviculum* is reliably distinguished from other *Phalium* species by possession of a specific combination of nucleotides in the sequence at sites 87 (G), 90 (C), 126 (T), 156 (G), 168 (A), 261 (A), 282 (C), 294 (A), 306

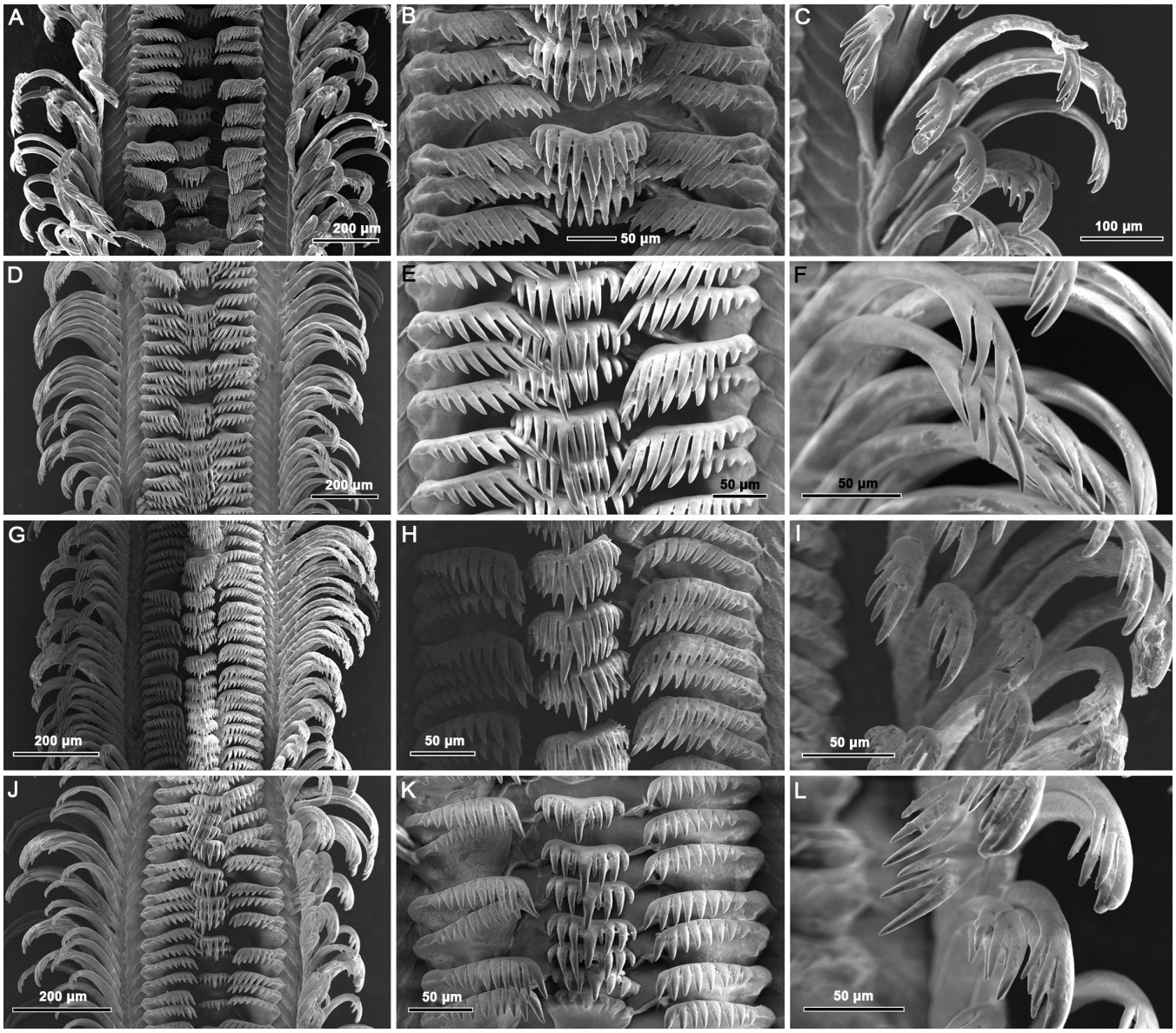

Figure 6. Radulae of *Phalium* species. **A**–**F**, *P. flammiferum* (Röding, 1798): (**A**–**C**) MBM288422, South China Sea, 60.8 mm; (**D**–**F**) MBM288426, East China Sea, 63.5 mm. **G**–**L**, *P. breviculum* Tsi & Ma, 1980: (**G**–**I**) MBM288432, Yellow Sea, off Qingdao, 47.0 mm; (**J**–**L**) MBM288442, Bohai Sea, off Laizhou, 54.6 mm. **A**, **D**, **G**, **J**, intact radula segment. **B**, **E**, **H**, **K**, central and lateral teeth. **C**, **F**, **I**, **L**, marginal teeth.

(G), 315 (T), 447 (A), 450 (T) and 490 (C).

Description. Shell (Fig. 5H–L) small for the genus (maximum height 64.8 mm), subglobose, relatively thin but solid. Spire low and conical; last whorl well inflated. Protoconch consisting of ~2.5 smooth, roundly convex whorls. Teleoconch of 6 whorls, with a weakly angled shoulder. Spiral cords and axial ribs on spire intersecting, giving surface a granulose appearance. On last whorl, spiral cords becoming much wider and rather flattened, 29–48 in number; axial sculpture limited to a few growth lines. In addition to spiral cords and axial ribs, shell surface bearing 1–3 prominent varices. Siphonal canal short and curved. Outer lip thickened, with 14–17 internal denticles; inner lip with well-developed parietal callus, forming a thick plait with tubercles on columella. Umbilicus covered by columellar plait. Shell colour white, adorned with longitudinal, curved, bright-brown streaks; outer lip, inner lip, and varices marked with obscure orange bands.

Radula (Fig. 6G–L) formula: 2.1.1.1.2. Central teeth bearing 3–6 long, strong denticles on each side of lon-

Figure 7. *Phalium breviculum* Tsi & Ma, 1980; live specimen in aquarium. Photograph by Jerry Dong.

ger and stronger central cusp. Lateral teeth each with 8–12 long, strong denticles, decreasing in size toward outer margin. Marginal teeth each bearing 3 or 4 denticles on inner edge.

Type locality. Yellow Sea, off Xiaochangshan Island, Dalian.

Geographic range. Distributed in the Bohai Sea and Yellow Sea, China, inhabiting sandy or muddy-sandy substrates at depths of 15–45 m. Based on published figures, this species may also occur in Korea and Japan (Min 2004; Okutani 2017).

Remarks. The shell morphology of *Phalium breviculum* has been well described in previous studies (Yen 1936; Tsi & Ma 1980; Zhang *et al.* 2016).

In terms of overall shell shape and colour pattern, this species is most similar to *Phalium flammiferum*. Nevertheless, *P. breviculum* can be distinguished from *P. flammiferum* in having more spiral cords on the body whorl (29–48 in *P. breviculum vs* 18–20 in *P. flammiferum*), and a reduced number of varices (1–3 in *P. breviculum vs* 3–5 in *P. flammiferum*). SEM observations of the radulae revealed clear intraspecific variation in the number of denticles on central, lateral, and marginal teeth among individuals of both species. The ranges of denticle number overlap between the two species, suggesting that radular characters are not suitable for delimiting the two species.

Discussion

Phalium breviculum was originally described as a subspecies of *Phalium flammiferum*, although it differs consistently from *P. flammiferum* in shell sculpture across all specimens examined and shows a distinct northern distribution in the present material, with no overlap with the sampled populations of *P. flammiferum*. However, Verbinnen *et al.* (2016)

argued that these differences are insufficient to warrant subspecific status for *P. breviculum* and synonymised it with *P. flammiferum*. The present study combing morphological and molecular evidence demonstrates that the differences are not intraspecific. Morphologically, the two species differ in spiral cords and varices. For molecular evidence, phylogenetic reconstructions based on concatenated COI + 28S rRNA sequences, as well as the tree inferred from COI gene, both recovered *P. flammiferum breviculum* as a distinct clade separate from *P. flammiferum flammiferum*. While the phylogeny generated from the 28S gene failed to recover monophyly for both *P. flammiferum breviculum* and *P. flammiferum flammiferum*, the two taxa still did not cluster together. In any cases, *P. flammiferum breviculum* can be genetically separated from *P. flammiferum flammiferum*. Thus, we formally elevate *Phalium flammiferum breviculum* Tsi & Ma, 1980 to full species rank as *Phalium breviculum*. Nonetheless, the material examined in our study is relatively limited, only based on specimens collected from Chinese waters. Such limited sampling fails to fully reflect intraspecific variation, especially for the extensively distributed *P. flammiferum*, which occurs across the East China Sea, South China Sea, Japan, and the Philippines. It is worth noting that Verbinnen *et al.* (2016) reported the presence of intermediate shell morphotypes between Japanese and Chinese populations, which require further integrative taxonomic research to determine whether cryptic species exist.

In Chinese waters, the geographical distributions of *P. breviculum* and *P. flammiferum* exhibit a distinct north–south pattern of differentiation across the Yangtze Estuary, with a narrow overlap between 30°05′N and 32°00′N (Tsi & Ma 1980). The divergence process of these two species within Chinese waters is likely driven by the combined effects of the Yangtze Estuarine Plume and the Yellow Sea Cold Water Mass. Specifically, the low-salinity barrier and sedimentary environmental heterogeneity created by the Yangtze Estuarine Plume restrict larval dispersal and gene flow. The low-temperature characteristics of the Yellow Sea Cold Water Mass further compress the ecological space for the southward expansion of *P. breviculum*. Notably, *P. breviculum* may also occurs in Japan (Okutani 2017), whereas no specimens from this region were examined in the present study. Therefore, we cannot currently draw definitive conclusions regarding the drivers of distributional divergence across the entire distribution range of these two species.

Cassids are moderately to very large, and most of them live on shallow, sandy substrates throughout much of the world's tropical and temperate oceans. However, molecular information of this group is very limited. Traditional taxonomy of this group was based primarily on shell morphology alone. Due to high variation in shell size and sculpture, there are few reliable characters that allow clear-cut specific distinction, resulting in taxonomic confusions at both the specific and the generic level (Beu 2008). In this study, in addition to *P. breviculum* and *P. flammiferum*, we also included COI and 28S sequences of *Phalium muangmani* to provide more molecular data for further taxonomic studies. Although PCA reveals measurable differences in shell morphology, these differences are primarily expressed as continuous variation, especially in shell outline. The mapping of shell landmark configurations onto the phylogeny further suggests that shell outline variation in *Phalium* is not tightly coupled with the inferred phylogenetic relationships. This weak correspondence is biologically informative and indicates that shell outline may evolve gradually and be affected by continuous variation. Therefore, overall shell outline should be interpreted cautiously in species delimitation. In contrast, discrete shell characters, especially the number of spiral cords on the last whorl and the number/development of varices, remain more useful for distinguishing *P. breviculum* from *P. flammiferum* in the present material. We expect that the use of integrative taxonomic approach, as applied in the present work, will play a significant role in improving the biodiversity knowledge of family Cassidae.

Acknowledgements

We are grateful to Yapeng Wang (Beijing Daheng Image Vision Co., Ltd), Xiaodong Chen (Qingdao, China), Erdong Chen (Dalian University of Technology), and Nan Chen (Taizhou, China) for their support in the acquisition of part of the specimens, and to Jerry Dong (Shenyang, China) for providing photographs of a living specimen. We also thank Jialei Chen (Capital Normal University) for providing support for the geometric morphometric analyses. We sincerely thank the editor, Robert Forsyth, the associate editor, Guoyi Zhang, and three anonymous reviewers for their constructive comments and valuable suggestions, which greatly improved this manuscript. This research work was funded by the National Key Research and Development Program of China (2024YFB4206600), the Independent Deployment Project of the Institute of Oceanology, Chinese Academy of Sciences (IOCASZZZX201), and the Biological Resources Programme of Chinese Academy of Sciences (CAS-TAX-24-031).

References

Beu AG. 2008. Recent deep-water Cassidae of the world: a revision of *Galeodea*, *Oocorys*, *Sconsia*, *Echinophoria* and related taxa, with new genera and species (Mollusca, Gastropoda). In: Héros *et al.* (Eds). *Tropical Deep-Sea Benthos, 25. Mémoires du Muséum national d'Histoire naturelle, Paris* **196**: 269–387.

Capella-Gutiérrez S, Silla-Martínez JM, Gabaldón T. 2009. trimAl: a tool for automated alignment trimming in large-scale phylogenetic analyses. *Bioinformatics* **25**: 1972–1973. doi: 10.1093/bioinformatics/btp348

Collin R. 2003. Phylogenetic relationships among calyptraeid gastropods and their implications for the biogeography of marine speciation. *Systematic Biology* **52**: 618–640. doi: 10.1080/10635150390235430

De Queiroz K. 2007. Species concepts and species delimitation. *Systematic Biology* **56**: 879–886. doi: 10.1080/10635150701701083

Fedosov A, Olivera BM, Watkins M, Barkalova V. 2014. A new species of *Casmaria* H. Adams & A. Adams, 1853 (Gastropoda, Cassidae) from the Philippines identified by molecular data. *European Journal of Taxonomy* **78**: 1–13. doi: 10.5852/ejt.2014.78

Gmelin JF. 1791. *Caroli a Linné Systema Naturae*, ed. 13, Tome 1(6): Vermes. G.E. Beer, Leipzig, pp. 3021–3910.

Goloboff PA, Morales ME. 2023. TNT version 1.6, with a graphical interface for MacOS and Linux, including new routines in parallel. *Cladistics* **39**: 144–153. doi: 10.1111/cla.12524

Jovelin R, Justine JL. 2001. Phylogenetic relationships within the polyopisthocotylean monogeneans (Plathyhelminthes) inferred from partial 28S rDNA sequences. *International Journal for Parasitology* **31**: 393–401. doi: 10.1016/S0020-7519(01)00114-X

Kalyaanamoorthy S, Minh BQ, Wong TKF, von Haeseler A, Jermiin LS. 2017. ModelFinder: fast model selection for accurate phylogenetic estimates. *Nature Methods* **14**: 587–589. doi: 10.1038/nmeth.4285

Klingenberg CP. 2011. MorphoJ: an integrated software package for geometric morphometrics. *Molecular Ecology Resources* **11**: 353–357. doi: 10.1111/j.1755-0998.2010.02924.x

Link DHF. 1807. *Beschreibung der Naturalien-Sammlung der Universität zu Rostock*, Part 3. Adlers Erben, Rostock, p. 112.

Min DK, Lee JS, Koh DB, Je JG. 2004. *Mollusks in Korea*. Min Molluscan Research Institute, Seoul, 566 pp.

Okutani T. 2000. *Marine Mollusks in Japan*. Tokai University Press, Tokyo, 1173 pp.

Okutani T. 2017. *Marine Mollusks in Japan, 2nd Edition*. Tokai University Press, Tokyo, 1375 pp.

Poppe GT. 2008. *Philippine Marine Mollusks, I*. ConchBooks, Hackenheim, 759 pp.

Puillandre N, Brouillet S, Achaz G. 2021. ASAP: Assemble Species by Automatic Partitioning. *Molecular Ecology Resources* **21**: 609–620. doi: 10.1111/1755-0998.13281

Qi ZY, Ma XT, Wang ZR, Lin GY, Xu FS, Dong ZZ, Li FL, Lü DH. 1989. *Mollusca of Huanghai and Bohai*. Agricultural Publishing House, Beijing, 309 pp.

Rambaut A, Drummond AJ, Xie D, Baele G, Suchard MA. 2018. Posterior summarization in Bayesian phylogenetics using Tracer 1.7. *Systematic Biology* **67**: 901–904. doi: 10.1093/sysbio/syy032

Ronquist F, Teslenko M, van der Mark P, Ayres DL, Darling A, Höhna S, Larget B, Liu L, Suchard MA, Huelsenbeck JP. 2012. MrBayes 3.2: efficient Bayesian phylogenetic inference and model choice across a large model space. *Systematic Biology* **61**: 539–542. doi: 10.1093/sysbio/sys029

Röding PF. 1798. *Museum Boltenianum, Pars secunda continens Conchylia sive Testacea univalvia, bivalvia & multivalvia*. Johan. Christi. Trappii, Hamburg, 199 pp. doi: 10.5962/bhl.title.16250

Rohlf FJ. 2021. tpsDig, digitize landmarks and outlines, version 2.32. https://www.sbmorphometrics.org/soft-dataacq.html.

Sansone C, Balestra C, Pistelli L, Del Mondo A, Osca D, Brunet C, Crocetta F. 2022. A comparative analysis of mucus immunomodulatory properties from seven marine gastropods from the Mediterranean Sea. *Cells* **11**: 2340. doi: 10.3390/cells11152340

Setiamarga DHE, Shimizu M, Nakashima S, Osaki C, Hirota K, Anggraeni L, Van Tu D, Sasaki T. 2025. DNA barcoding of museum-vouchered samples collected from fish markets reveals an unexpected diversity of consumed gastropods in Vietnam. *Future Foods* **12**: 100689. doi: 10.1016/j.fufo.2025.100689

Strong EE, Puillandre N, Beu AG, Castelin M, Bouchet P. 2019. Frogs and tuns and tritons—a molecular phylogeny and revised family classification of the predatory gastropod superfamily Tonnoidea (Caenogastropoda). *Molecular Phylogenetics and Evolution* **130**: 18–34. doi: 10.1016/j.ympev.2018.09.016

Sun Y, Li Q, Kong L, Zheng X. 2012. DNA barcoding of Caenogastropoda along coast of China based on the COI gene. *Molecular Ecology Resources* **12**: 209–218. doi: 10.1111/j.1755-0998.2011.03085.x

Talavera G, Castresana J. 2007. Improvement of phylogenies after removing divergent and ambiguously aligned blocks from protein sequence alignments. *Systematic Biology* **56**: 564–577. doi: 10.1080/10635150701472164

Tanura K, Stecher G, Peterson D, Filipski A, Kumar S. 2013. MEGA6: Molecular Evolutionary Genetics Analysis version 6.0. *Molecular Biology and Evolution* **30**: 2725–2729. doi: 10.1093/molbev/mst197

Tsi CY, Ma ST. 1980. Étude sur les espèces des Cassidae de la Chine. *Studia Marina Sinica* **16**: 83–96.

Verbinnen G, Segers L, Swinnen F, Kreipl K, Monsecour D. 2016. *Cassidae – an Amazing Family of Seashells*. ConchBooks, Harxheim, 251 pp.

Xie JM, Chen YR, Cai GJ, Cai RL, Hu Z, Wang H. 2023. Tree Visualization By One Table (tvBOT): a web application for visualizing, modifying and annotating phylogenetic trees. *Nucleic Acids Research* **51**: W587–W592. doi: 10.1093/nar/gkad359

Yen TC. 1933. The molluscan fauna of Amoy and its vicinal regions. *Report of the Marine Biological Association of China* **2**: 1–120.

Yen TC. 1936. Marine Gastropoda of Shantung Peninsula. *Contributions from the Institute of Zoology, National Academy of Peiping* **3**: 165–255.

Zhang SP, Ma XT. 2004. *Fauna Sinica. Invertebrata, Vol. 34: Mollusca, Gastropoda, Tonnacea*. Science Press, Beijing, 249 pp.

Zhang SP, Zhang JL, Chen ZY, Xu FS. 2016. *Mollusks of the Yellow Sea and Bohai Sea*. Science Press, Beijing, 421 pp.

Zhang SP, Zhang SQ. 2015. Types of marine gastropods deposited in the Marine Biological Museum, Chinese Academy of Sciences. *Shell Discoveries* **1**: 3–19.

Zhao RY. 1982. *Marine Mollusks of Dalian*. Ocean Press, Beijing, 167 pp.

Supplemental Materials

Supplementary file (doi: 10.61733/jconch/4579s) containing additional figures:

Figure S1. Mapping of shell landmark configurations onto the molecular phylogeny of three *Phalium* species

Figure S2. Phylogenetic tree inferred by Bayesian analysis (BI) from sequences of COI gene.

Figure S3. Phylogenetic tree inferred by Bayesian analysis (BI) from sequences of 28S gene

Figure S4. The 10 best partitions inferred by the Assemble Species by Automatic Partitioning (ASAP).

Manuscript submitted: 1 April 2026
Revised manuscript accepted: 6 July 2026
Associate Editor: Guoyi Zhang